Multistatic Radar Processing and Systems

Chris J. Baker
College of Engineering and Computer science, ANU
e-mail: chris.baker@anu.edu.au

Keywords: radar, multistatic radar, multistatic radar, distributed sensing, waveforms, ambiguity

Multistatic Radar Sensitivity

Radar sensitivity, usually defined in terms of signal to noise ratio (SNR), is perhaps the most important parameter used to evaluate the performance of a radar system, as it indicates the radar's ability to detect the presence of a target. Normally the minimum acceptable SNR is defined by the required probability of detection and the probability of false alarm. Radar sensitivity is affected by many factors, such as transmitted power, antenna gain, transmitted wavelength, etc, which can be managed by radar designers, and other factors, such as target cross section, target distance from radar receivers, etc, which depend on the surveillance scenario. Monostatic sensitivity can be calculated by the conventionally used monostatic radar equation [45].

The multistatic form of the radar equation is developed here to evaluate multistatic radar sensitivity properties. A fully coherent radar network is considered, which means that the radars comprising the whole network have a common and highly precise knowledge of time and space. The whole radar network is composed of m transmitters and n receivers. It is assumed that the whole network is well synchronized and works cooperatively such that each receiver is capable of receiving echoes due to any transmitters in the network. It is also assumed that the target is an isotropic radiator, giving a constant RCS in all directions. Under these assumptions, it is reasonable to calculate the overall radar sensitivity by summing up the partial signal to noise ratio, which is given by:

$$SNR_{netted} = \sum_{i=1}^{m} \sum_{j=1}^{n} \frac{P_{ti} G_{ti} G_{rj} \sigma_{ij} \lambda_i^2}{(4\pi)^3 k T_s B_i R_{ti}^2 R_{rj}^2 L_{ij}} \qquad (1)$$

Where

P_{ti} = i th transmitted power
G_{ti} = i th transmitter gain
G_{rj} = j th receiver gain
σ_{ij} = radar cross section (RCS) of the target for i th transmitter j th receiver
λ_i = i th transmitted wavelength
T_s = receiving system noise temperature
B_i = bandwidth of the matched filter for the i th transmitted waveform
L_{ij} = system loss for i th transmitter, j th receiver
R_{ti} = distance from i th transmitter to target
R_{rj} = distance from target to j th receiver

Considering the simplest case where the radar parameters for every transmitter-receiver combination are the same, the multistatic radar equation can be simplified as:

$$SNR_{netted} = \frac{P_t G_t G_r \sigma \lambda^2}{(4\pi)^3 k T_s B L} \sum_{i=1}^{m} \sum_{j=1}^{n} \frac{1}{R_{ti}^2 R_{rj}^2} \qquad (2)$$

From this equation, it is clear to see that the multistatic radar geometry, i.e. the positions of target and radar nodes in the network, will have great influence on the overall multistatic radar sensitivity.

A simulation has been developed in Matlab allowing a range of radar and geometrical parameters to be input. The key variable parameters in this simulation are shown in table 2.

PARAMETER	VALUE
Pt (W)	6000
Gt (db)	30
Gr (db)	30
λ (m)	0.1
σ (m^2)	10
L (db)	5

Table2: Parameters used for sensitivity simulations

Fig.15 shows the detection range of a monstatic radar using the parameters from Table 2. This in both two dimensional and three dimensional surveillance geometries. The detection threshold has been set as 13 db. This provides the detection probability of 0.85 for a false alarm probability of 10^{-6}. It is shown that monostatic radar gives a spherical sensitivity iso-surface in three dimensional space, whereas a circular contour in two dimensions. This is the direct result of isotropic transmission of radiated energy.

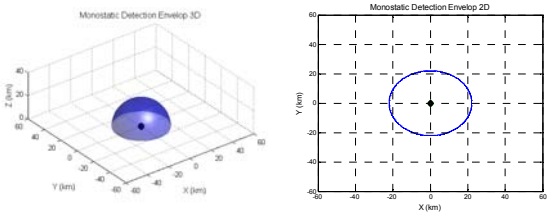

Figure 15. 3D and 2D monostatic radar sensitivitiy

A range of multistatic radar simulations now follow. The radar network is composed of three transmitters and three receivers. The total transmitted power of 6kw is evenly distributed among all three transmitters. All the other key parameters remain the same as the monostatic examples. This forms the simplest multistatic radar model, and therefore, the multistatic radar sensitivity can be calculated by (2).

In Fig. 16, the three transmitters and receivers are all co-located. It is shown that the shapes of coverage maps are similar to the monostatic case. Although the total transmitted power is the same as the monostatic one, the coverage area is enlarged. This is because each receiver accepts echoes from every

transmitter, giving an increase in the totally received power and therefore enlarged coverage area. Clearly multistatic radar makes better use of the available transmitter power than a monostatic system.

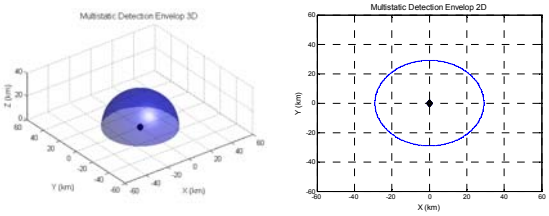

Figure 16. 3D and 2D multistatic radar sensitivity-collocated transmiters and receivers

Fig. 7 shows the sensitivity plots of multistatic radar with fully dispersed nodes. In this case, the whole system is effectively composed of nine bistatic pairs. It can be seen that, compared to the co-located transmitter and receiver scenario, the coverage area in the first two dimensions are enlarged, and at the same time it is dramatically reduced in the third dimension of height. This is expected, as the total transmitted power remains the same.

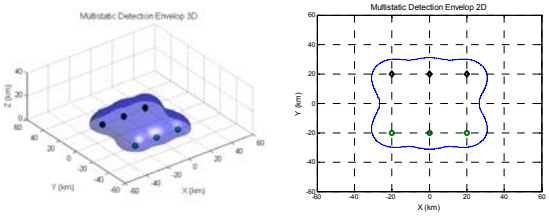

Figure 17. 3D and 2D multistatic radar sensitivity-dispersed transmitters and receivers

Asymmetrically distributed multistatic radar sensitivity plots are shown in Fig. 18, where the two monostatic radars are positioned at the bottom part of the map, while a single transmitter and a single receiver are positioned separately at the top part of the map. This forms a radar network with two monostatic and seven bistatic radars. The asymmetrical coverage maps are shown due to the asymmetrical distribution of the transmitted energy. The coverage is more concentrated on the bottom part of the area in three dimensions, due to the more radar nodes distributed in this area.

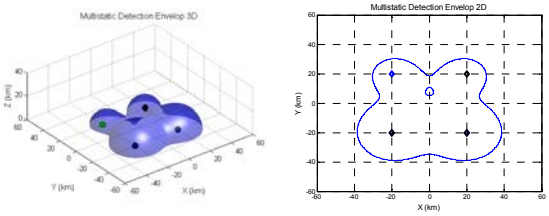

Figure 18. 3D and 2D multistatic radar sensitivity-asymmetrically distributed transmitters and receivers

Overall the great range of the form of the results shows the variablility of coverage that can be generated. This illustrate the extra design freedom of multistatic radar that can be used to tailor coverage to a given application. We also note that in the case where the ERP is a constant that extended ground coverage is at the expense of coverage in height.

The multistatic radar ambiguity function

It is widely recognised that the ambiguity function is an important tool to evaluate radar performance in terms of target resolution and clutter rejection. The concept of ambiguity function was firstly defined by *Woodward* [40]. It can be seen as the absolute value of the envelope of the output of a matched filter when the input to the filter is a Doppler shifted version of the original transmitted signal, to which the filter is matched . If *u (t)* is the complex envelop of the transmitted signal, the ambiguity function is calculated by:

$$\left|\chi(\tau, f)\right| = \left|\int_{-\infty}^{+\infty} u(t)u^*(t-\tau)e^{j2\pi ft}dt\right| \qquad (3)$$

Monostatic radar ambiguity is fairly well developed, and a variety of examples can be found in literature [41]. Bistatic radar ambiguity is developed by *Tsao et al.*[42].

The multistatic radar ambiguity function is formulated based on the bistiatic radar ambiguity calculation. It is assumed that the radar network is composed of N transmitters and one single receiver, such that it is easy to choose the receiver as the common reference point. In this case the radar network comprises N bistatic pairs. The analysis is based on the matched filter processing at the receiver.
There are some important assumptions for the formulation of multistatic radar ambiguity function. Firstly, the target is slowly fluctuating and its scattering properties do not change with the look angles. Secondly, the transmitted signals are the same and the filter is matched to the original transmitted signal. A very important assumption is that the network is coherent. This implies that the echoes arriving at different time instances can be processed jointly. Similar to the bistatic radar ambiguity analysis, the multistatic radar ambiguity function is developed by the following three steps:

- To calculate bistatic ambiguity function for each transmitter-receiver pair by (3).
- To calculate weighting factor according to received signal intensity.

$$P_{ri} = \frac{P_{ti}G_{ti}G_r\lambda^2\sigma}{(4\pi)^3(R_{ti}R_r)^2}, i = 1,2...N \qquad (4)$$

$$w_i = \frac{P_{ri}}{Max(P_{ri})} \qquad (5)$$

- To formulate multistatic radar ambiguity function using the results form previous calculations:

$$\chi_{netted} = \left|\sum_{i=1}^{N} w_i\chi_i\right|^2 \qquad (6)$$

Here, a three dimensional multistatic radar model has been developed for a comprehensive understanding of multistatic radar ambiguity performance. It is assumed that the fixed transmitters and receiver are located in one plane and the target is moving in another plane which is parallel to the transmitter-receiver plane. An example three dimensional multistatic radar system geometry, used for the multistatic radar ambiguity analysis is shown in Fig. 19.

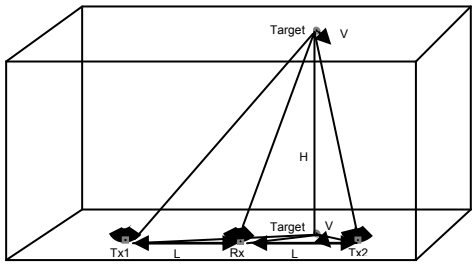

Figure 19. 3D multistatic radar system geometry

A vectorial approach is used to calculate the two important parameters, delay and Doppler, which are used for ambiguity function calculation.

$$\tau = \frac{\left|\overrightarrow{R_t}\right| + \left|\overrightarrow{R_r}\right|}{c} \tag{7}$$

$$f_b = \frac{1}{\lambda}\left[\frac{d}{dt}(\overrightarrow{R_t} + \overrightarrow{R_r})\right] = \frac{1}{\lambda}\left[\frac{\overrightarrow{R_t}\cdot\vec{V}}{\left|\overrightarrow{R_t}\right|} + \frac{\overrightarrow{R_r}\cdot\vec{V}}{\left|\overrightarrow{R_r}\right|}\right] \tag{8}$$

The signal used for the multistatic radar ambiguity function simulation is a coherent pulse train consisting of three rectangular pulses with 40 μs pulse length, 100 μs period, and carrier frequency ω_c =3×10^8 rad/s. The target is flying within a surface which is parallel to ground with 600 m/s velocity. Only target close to baseline cases are simulated here, because this is where the degradation of ambiguity properties appears in bistatic cases.

The multistatic radar ambiguity function is plotted in a range-velocity plane rather than the traditional delay-Doppler plane, because these two are the primary parameters of interest, and only in this way the influence of system geometry on ambiguity properties can be shown. Ambiguity function contour and cuts along range and velocity axes are presented, where the width of the main peaks represent range and velocity resolutions.

In the first group of simulations, the baseline is 10 km; the target is 6 km far from the receiver for the two dimensional simulation. The system geometry used for Fig. 20-22 is shown in Fig. 5, where two transmitters are positioned on two sides of a common receiver with the same baseline length. Two dimensional multistatic radar ambiguity diagrams are shown in Fig. 20. It is observed that, in two-dimensional case, when the target is close to bistatic baseline, range and velocity resolutions are degraded dramatically.

Fig. 21 and Fig. 22 show the three dimensional multistatic radar ambiguity diagrams with target height of 20km and 4km, respectively. In Fig. 21, the target is far from the transmitter-receiver plane. Both range and velocity resolutions are improved greatly, forming a relatively sharp peak in range and velocity domain, respectively. However, when the target is not far enough from the transmitter-receiver plane, this improvement is considerable less (Fig. 22).

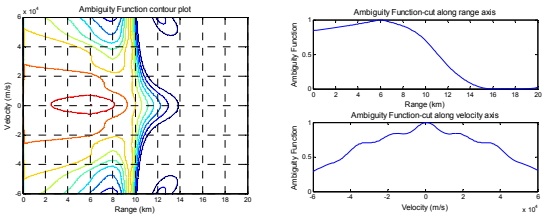

Figure 20. 3D multistatic radar ambiguity function

Figure 1.

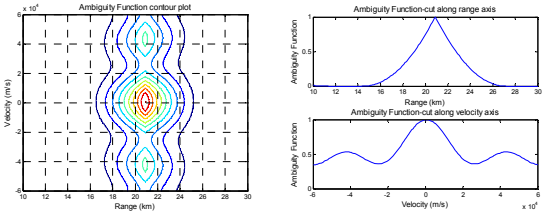

Figure 21. 3D multistatic radar ambiguity function-H = 20 km

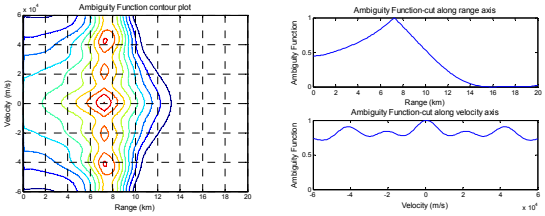

Figure 22 3D multistatic radar ambiguity function-H = 4 km

For the next stage, two more transmitters were added to the multistatic radar system to form a multistatic radar system with four transmitters and one receiver, effectively, four bistatic radar pairs. This system geometry is shown in Fig. 23 in two dimensions. Other parameters remain the same as former examples. Fig. 24 shows that when more radar nodes are applied, the three dimensional range and velocity resolutions are further improved compared with the two transmitters case.

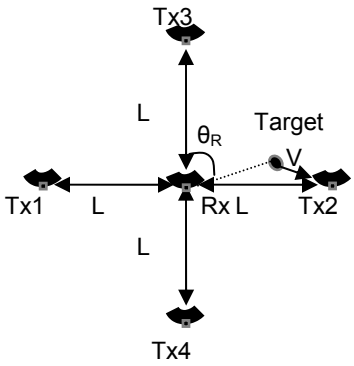

Figure 23. 2D multistatic radar geometry-4 transmitters

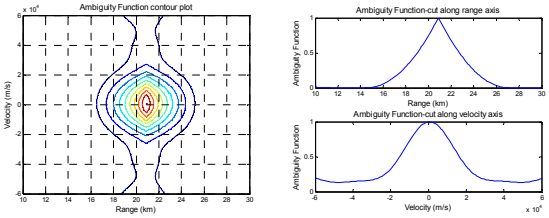

Figure 24. 3D multistatic adar ambiguity function-4transmitters H=20km

The final example shows the multistatic radar ambiguity diagrams with a shorter baseline. In this case, the baseline length is 1 km; target is 600m from the receiver for the two dimensional simulation; the target height is 4 km for three dimensional geometry. Other parameters remain the same as former examples. From Fig. 25 one can observe that regardless of the baseline length, when the target is close to baseline, the range and velocity resolutions are degraded. The three dimensional multistatic radar ambiguity diagrams of this system geometry are shown in Fig. 26. It illustrates that in the short baseline case, the three dimensional multistatic radar geometry with 4 km target height can provide the improvement of range and velocity resolutions comparable to the 20 km target height of long baseline case which is shown in Fig. 21. Clearly, the target height to baseline length ratio appears to play an important role in the three dimensional multistatic radar ambiguity function and thus system performance.

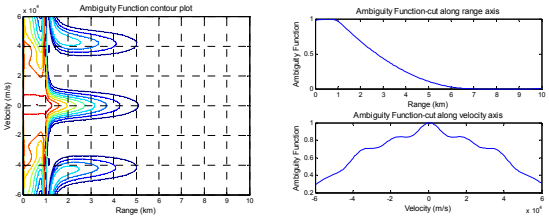

Figure 25. 2D multistatic radar ambiguity function-short baseline

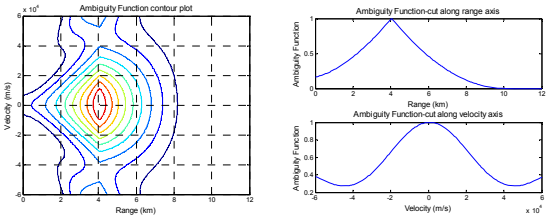

Figure 26. 3D multistatic radar ambiguity function-shor baseline H=4km

Conclusions

It has been shown that multistatic radar sensitivity is not only dependent on radar parameters, but also on system geometry. Multistatic radar offers more flexible arrangement of system geometry than traditional monostatic radar, providing the possibility to configure radar nodes to form a satisfactory coverage area.

It has also been shown that the multistatic radar ambiguity function is strongly dependent on the specific multistatic radar system geometry. When the target is close to the bistatic baseline, large ambiguities are found in the two dimensional cases. The three dimensional geometry has a significant effect on the ambiguity properties, where the target height to baseline length ratio is the dominant factor, and smaller baselines performs better than longer baseline. Adding more radar nodes gives more flexible multistatic radar system geometry and provides the possibility to further improve multistatic radar resolution capability.

Overall multistatic radar has many advantages but these do come at the cost of an increased complexity. Additionally, this is a far from mature form of sensing and there remains much research and development to be done if multistatic radar is to find routine operational use.

References

[1] Willis, Nicholas J., 'Bistatic Radar', *Artech House Inc.*, 1991
[2] Chernyak, V.S., 'Fundamentals of Multisite Radar Systems', *Gordon and Breach Science Publishers*, 1998
[3] Cameron, A., 'The Jindalee operational radar network: its architecture and surveillance capability', *Radar Conference 1995*, pp 692-697, May 1995
[4] Beide, W., 'The nature of Bistatic and Multistatic Radar', *International conference on Radar*, 15-18 Oct. 2001
[5] Yongguang, C., Xicheng, L., Hua, Q., Xiaojun, J., 'On study of the application of ATM switches in multistatic-radar systems', *Aerospace and Electronics Conference*, Proc. of the IEEE,Vol. 2, 14-17 July 1997
[6] Thomopoulos, S.C.A., Okello, N.N., 'Design of a robust Multiradar Distributed Data Fusion System', *The First IEEE Regional Conference on Aerospace Control Systems*, pp599-603, May 25-27, 1993
[7] Swift, M., Riley, J.L., Lourey, S., Booth, L., 'An overview of the multistatic sonar program in Australia', *Fifth International Symposium on Signal Processing and Its applications*, Vol. 1, Aug. 1999
[8] Que W., Peng Y., LuD., Hou X., 'A new approach to data fusion for stealth targets tracking', *Radar* 97, pp657-661, Oct. 1997
[9] Jinlei, J., Hongbin, R., Fuli, G., Huaisuo, D., 'A Preliminary Research into the Multistatic Radar Seekers for Anti-stealth Aircraft', *Fourth International Conference on Signal Processing*, Vol. 2, 12-16 Oct. 1998
[10] Fischer C., Younis M., Wiesbeck W., 'Multistatic GPR data acquisition and imaging'. *IEEE International Geoscience and Remote Sensing Symposium*, pp328-330, June 2002
[11] Johnsen, T., Olsen, K.E., Gundersen, R., 'Hovering Helicopter measured by Bi-Multistatic CW Radar', *IEEE Conference on Radar*, pp165-170, 5-8 May 2003
[12] Celldar, http://: www.roke.co.uk/sensors/stealth/celldar.asp
[13] Horne, A.M., Yates, G., 'Bistatic Synthetic Aperture Radar', RADAR 2002, 15-17 Oct. 2002
[14] Soumekh, M, "Bistatic synthetic aperture radar imaging using wide-bandwidth continuous-wave source", Proceedings of the Society of Photo-Optical Instrumentation Engineers (SPIE), 1998, pp. 99-109
[15] Cherniakov, M., Kurt, K., and Nezlin, D., "Bistatic Synthetic Aperture Radar with Non-Cooperative LEOS Based Transmitter", IEEE Geoscience and Remote Sensing Symposium 2000, Vol. 2, pp. 861-862
[16] Whitewood, A.P., Müller, B.R., Griffiths, H.D., and Baker, C.J., "Bistatic Synthetic Aperture Radar with Application to Moving Target Detection", Proceedings of the IEEE International Conference on Radar 2003, Adelaide, Australia
[17] Seliga, T.A., Coyne, F.J., 'Multistatic Radar as a means of Dealing with the Detection of Multipath False Targets by Airport Surface Detection Equipment Radars', *IEEE Conference on Radar*, pp329-336, 5-8 May 2003
[18] Evers C., Smith A., 'Innovative radar multistatic techniques for air traffic control', The 19th Digital Avionics Systems Conferences, Vol. 2, pp7B2/1-7B2/7, Oct. 2000
[19] Groll, H.P., Detlesfen, J., Siart, U., 'Multisensor Systems at mm-Wave Range for Automotive Applications', Oct. 2001

[20] Rohling, H., Hob, A., Lubbert, U., Schiementz. 'Multistatic Radar Principles for Automotive RadarNet Applications', *German Radar Symposium*, Sept. 2002
[21] Hall, C.D., Cordey, R.A., 'Multistatic Scatterometry', *International Geoscience and Remote Sensing Symposium*, Vol. 1, pp561-562, 12-16 Sept. 1988
[22] Soumekh M., 'Multistatic Echo Imaging in Remote Sensing and Diagnostic Medicine'. *Multidimensional Signal Processing Workshop*, pp200, *Sept*. 1989
[23] Winter, J.E., Anderson, N.C., 'Distributed Aperture implementation on the TechSat 21 Satellites', *Aerospace Conference*, IEEE Proc., March 8-15, 2003
[24] IEE Proceedings on Bistatic and Multistatic Radar, Part F, Dec. 1986
[25] Williamson, F.R., Brooks, R., Greneker, E.F., Currie, N.C., Williamson, J., McGee, M.C., 'Radar as part of a multistatic surveillance system – A problem revisited', *International Carnahan Conference on Security Technology*, pp14-18, 14-16 Oct. 1992
[26] Gini, F., Lombardini, F., Verrazzani, L., 'Robust monoparametric multiradar CFAR detection against non-Gaussian spiky clutter', *Radar, Sonar and Navigation*, IEE Proc., Vol. 144, Issue 3, pp131-140, June 1997
[27] **'**Modeling and Simulation Air-Defence Radar Network under Saturation Attack', http://doppler.unl.edu/~rockee/sim/sim.htm
[28] Wenlin, Y., Chongyu, W., 'Target location and speed estimation by multistatic radar system using maximum likelihood approach', *5th International Conference on Signal Processing*, Vol. 3, pp1964-1967, 21-25 Aug. 2000
[29] Baumgarten D. Optimum detection and receiver performance for multistatic radar configurations. May 1982
[30] Xing, H.L., Zhongkang, S., 'Location and tracking technique in a multistatic system established by multiple bistatic systems', *Proceeding of the IEEE National Aeorspace and Electronics Conference*, Vol. 1, pp437-441, May 1991
[31] Griffiths, H. D., and Long, B. A., 'Television-based bistatic radar', *IEE Proceedings*, Vol. 133, Part F, No.7, pp649-657, Dec. 1986
[32] Griffiths, H.D, Garnett, A.J., Baker, C.J., Keaveney, S., 'Bistatic Radar Using Satellite-Borne Illuminators of Opportunity', *Radar '92 International Conference*, pp276-279, Oct. 1992
[33] Wu, Y., Munson, D.C, Jr 'Multistatic Synthetic Aperture Imaging of Aircraft using Reflected Television Signals', *Algorithms for Synthetic Aperture Radar Imagery VIII*, Proc. SPIE, April 2001
[34] Wu Y., Munson D.C., Jr, 'Multistatic Passive Radar Imaging using Smoothed Pseudo Wigner-Ville Distribution', *International conference on Image Processing*, Vol. 3, pp604-607, Oct. 2001
[35] Silent Sentry, http://www.lockheedmartin.com/
[36] Koch V., Westphal R., 'A New approach to a Multistatic Passive Radar Sensor for Air Defence', *IEEE Aerospace and Electronic* Magazine, Vol. 10, Issue 11, pp24-32, Nov. 1995
[37] Steyskal H., Schindler J.K., Franchi P., Mailloux R.J., 'Pattern synthesis for TechSat 21 – A distributed Space-based radar system', *RADAR 2002*, pp375-379, Oct. 2002
[38] Gjessing, D.T., Saebboe, J., 'Characterization of objects and general ocean phenomena by use of target adaptive multifrequency multistatic illumination acoustics', Radar, Sonar and Navigation, IEE Proceedings, Vol. 149, Issue 2, pp60-69, April 2002
[29] Bath, W.G., 'Tradeoffs in Radar Networking', *RADAR 2002*, pp26-30, 15-17 Oct. 2002
[40] Woodward, P.M., 'Probability and Information Theory, with Applications to Radar', *Pergamon*, New York, 1953
[41] Levanon, N., 'Radar principles', *Wiley*, 1998

[42] Tsao, T., Slamani, M., Varshney, P., Weiner, D., Schwarzlander, H., 'Ambiguity function for a Bistatic Radar', *IEEE Transactions on Aerospace and Electronic Systems*, Vol. 33, Issue 3, pp1041-1051, July 1997
[43] Baker, C.J., Hume, A.L., 'Multistatic radar sensing', *IEEE Aerospace and Electronic Systems Magazine*, Vol. 18, Issue 2, pp3-6, Feb. 2003
[44] Levanon, N. Mozeon, E. 'Radar Signals' Wiley, 2004
[45] Kingsley, S. Quegan, S. Understanding Radar Systems, McGraw-Hill, 1992